Melting of Wigner crystal in high-mobility n-GaAs/AlGaAs heterostructures at filling factors 0.18>ν>0.125: Acoustic studies

I. L. Drichko, I. Yu. Smirnov, A. V. Suslov, Y. M. Galperin, L. N. Pfeiffer, and K. W. West

Phys. Rev. B **94**, 075420 — Published 15 August 2016

DOI: 10.1103/PhysRevB.94.075420

Melting of Wigner crystal in high-mobility n-GaAs/AlGaAs heterostructures at filling factors $0.18 > \nu > 0.125$: Acoustic studies.

I. L. Drichko,[1] I. Yu. Smirnov,[1] A. V. Suslov,[2] Y. M. Galperin,[3,1] L. N. Pfeiffer,[4] and K. W. West[4]

[1] *A. F. Ioffe Physico-Technical Institute of Russian Academy of Sciences, 194021 St. Petersburg, Russia*
[2] *National High Magnetic Field Laboratory, Tallahassee, FL 32310, USA*
[3] *Department of Physics, University of Oslo, 0316 Oslo, Norway*
[4] *Department of Electrical Engineering, Princeton University, Princeton, NJ 08544, USA*

(Dated: June 30, 2016)

Using acoustic methods the complex high-frequency conductance of high-mobility n-GaAs/AlGaAs heterostructures was determined in magnetic fields 12÷18 T. Based on the observed frequency and temperature dependences we conclude that in the investigated magnetic field range and at sufficiently low temperatures, $T \lesssim 200$ mK, the electron system forms a Wigner crystal deformed due to pinning by disorder. At some temperature, which depends on the electron filling factor, the temperature dependences of both components of the complex conductance get substantially changed. We have ascribed this rapid change of the conduction mechanism to melting of the Wigner crystal and study the dependence of the so-defined melting temperature on the electron filling factor.

PACS numbers: 73.63.Hs, 73.50.Rb

I. INTRODUCTION

Transport properties of a two-dimensional electron system (2DES) in high magnetic fields (B) are governed by an interplay between electron-electron interaction and their interaction with impurities. Both interactions depend on the typical size of the electron wave function, which is parameterized by the magnetic length, $l_B = \sqrt{c\hbar/eB}$. At high B, $l_B \to 0$ and electrons act as classical point particles. Without disorder, such particles tend to form a triangular lattice - a Wigner crystal (WC) - stabilized by electron repulsion.[1] The wave function overlap decreases with increase of B. Its role is quantitatively characterized by the ratio between l_B and the lattice constant, a, of the WC. The ratio l_B/a is related to the Landau filling factor, ν, as $\nu = nh/eB = (4\pi/\sqrt{3})(l_B/a)^2$. At sufficiently high ν the WC ground state is predicted to undergo a transition to the fractional quantum Hall effect (FQHE) state, see, e.g., Ref. 2 for a review.

Since 2DESs at high magnetic fields are insulators it is concluded that WC is pinned by disorder. The disorder leads to texturing of the electron system into domains, typical size L of which (the so-called Larkin-Ovchinnikov length) can be estimated comparing the cost in shear elastic energy and the gain due to disorder.[3] This conclusion is supported by observation of well-defined resonances in the microwave absorption spectrum.[4,5] In the pinning mode, parts of WC oscillate within the disorder-induced potential, which defines the so-called pinning frequency, ω_p.

These oscillations get mixed with the cyclotron motion in the magnetic field resulting in absorption peaks at some frequencies, f_{pk}.[6–8] In the classical, high-B limit, where l_B is much smaller than any feature of the disorder, and also small enough that the wave function overlap of neighboring electrons can be neglected, $f_{pk} \propto B^{-1}$.

The perfection of the WC order in 2DES has been addressed previously using time-resolved photoluminescence[9] provided evidence for triangular crystalline ordering in the high-B regime. In double quantum wells, evidence for ordering came from commensurability effects.[10] In the context of the model described in Ref. 8, the domain size has been estimated previously from early microwave,[11] surface acoustic wave,[12] and nonlinear I-V data.[11,13]

Previously[14] we have studied dependences of complex conductance, $\sigma^{AC}(\omega) \equiv \sigma_1(\omega) - i\sigma_2(\omega)$, on frequency, temperature, and magnetic field in the vicinity of the filling factor 1/5, namely for $0.19 < \nu < 0.21$. The complex conductance was extracted from simultaneous measurements of magnetic field dependences of attenuation and variation of velocity of surface acoustic waves (SAW) propagating in the vicinity of the sample surface. The results were interpreted as evidence of formation of a pinned Wigner crystal (WC). This conclusion was based on an observed maximum in the frequency dependence of σ_1 at $f \equiv \omega/2\pi \sim 100$ MHz coinciding with a change of the sign of $\sigma_2(\omega)$. This results allowed us to estimate the domain size in the pinned WC.

In this paper we study the dependences of complex conductance on the frequency, the temperature and the SAW electric field intensity in the same structure, but in higher magnetic field $12 < B < 18$ T corresponding to $0.18 > \nu > 0.125$, respectively. The measurements are made for temperatures $T = (40 \div 340)$ mK and SAW frequencies $f = (30 \div 300)$ MHz.

The paper is organized as follows. In Sec. II A we describe the experimental setup and the samples. The experimental results are reported in Secs. II B and II C. They are discussed in Sec. III.

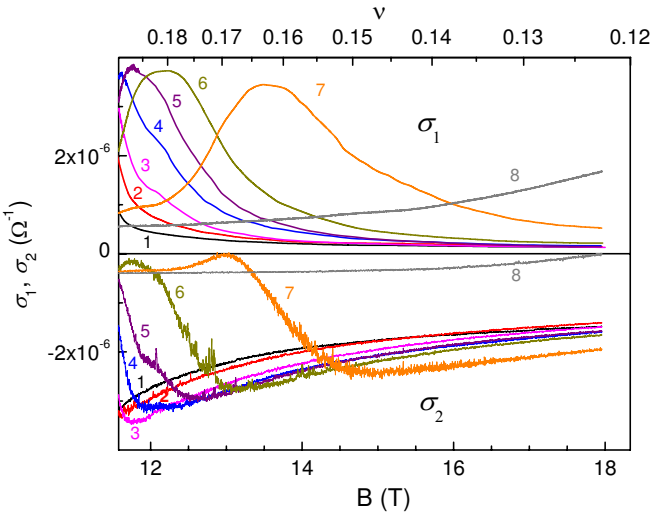

FIG. 1. (Color online) Magnetic field dependences of σ_1 and σ_2 for different temperatures, T, mK: 1 - 40, 2 - 74, 3 - 87, 4 - 100, 5 - 112, 6 - 122, 7 - 160, 8 - 240; $f = 28.5$ MHz.

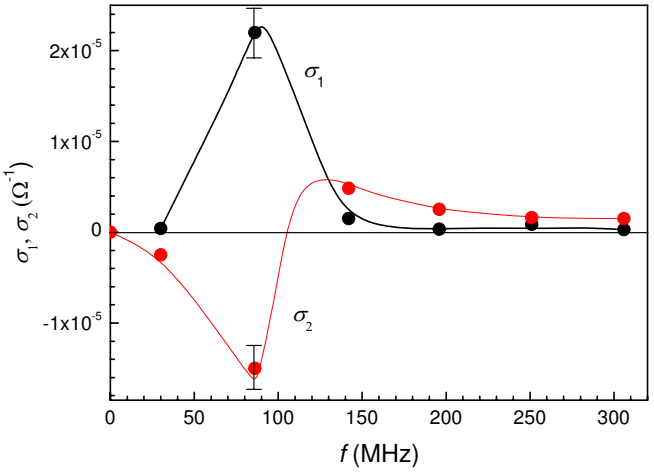

FIG. 2. Frequency dependences of σ_1 and σ_2 at $T = 40$ mK and $\nu = 0.18$ ($B = 12.2$ T). Lines are guides for an eye.

II. EXPERIMENTAL PROCEDURE AND RESULTS

A. Experimental setup and sample

As previously,[14] we use the so-called hybrid acoustic method discussed in detail in Ref. 15, see Fig. 1 (left) in that paper. A sample is pressed by springs to a surface of a $LiNbO_3$ piezoelectric crystal where two inter-digital transducers (IDTs) are formed. One of the IDTs is excited by AC pulses. As a result, a SAW is generated, which propagates along the surface of the piezoelectric crystal. The piezoelectric field penetrates into the sample and the in-plane longitudinal component of the field interacts with the charge carriers. This interaction causes SAW attenuation and deviation of its velocity.

We study multi-layered n-GaAlAs/GaAs/GaAlAs structures with a wide (65 nm) GaAs quantum well (QW), the same as in Ref. 14 (see right panel of Fig. 1 in that paper). The QW is δ-doped from both sides and is located at the depth d = 845 nm from the surface. The electron density is $n = 5 \times 10^{10}\text{cm}^{-2}$ and the mobility is $\mu_{0.3\text{K}} = 8 \times 10^6$ cm^2/V×s. Studies show that at the given electron density only the lowest band of transverse quantization should be occupied.[10]

B. Results: Linear response

Shown in Fig. 1 are the magnetic field dependences of σ_1 and σ_2 for $f = 28.5$ MHz extracted from simultaneous measurements of the SAW attenuation, Γ, and the relative variation of its velocity, $\Delta v/v$. These data were used for calculating the components of the complex conductance, $\sigma^{AC}(\omega) \equiv \sigma_1(\omega) - i\sigma_2(\omega)$, according to the procedure outlined in Ref. 15. Namely, the complex AC conductance $\sigma^{AC}(\omega)$ was calculated using Eqs. (1)-(7) from Ref. 15 where we substituted $\varepsilon_1 = 50$, $\varepsilon_0 = 1$ and $\varepsilon_s = 12$ for the dielectric constants of the $LiNbO_3$ crystal, of the vacuum and of the sample, respectively. The finite vacuum clearance $a = 5 \times 10^{-5}$ cm between the sample surface and the $LiNbO_3$ surface was determined from the saturation value of the SAW velocity in strong magnetic fields at $T = 380$ K; $d = 845$ nm is the finite distance between the sample surface and the 2DES layer. The SAW velocity is $v_0 = 3 \times 10^5$ cm/s.

The frequency dependences of the components σ_i shown in Fig. 2 is a characteristic of the Wigner crystal pinned by disorder with pinning frequency ~ 86 MHz in this case.

Shown in Fig. 3 are the frequency dependences of σ_1 for different filling factors. The curves have maxima at $f \approx 86$ MHz, their amplitudes are decreasing when the magnetic field increases, see inset.

The same σ_1 data are presented in Fig. 4 as the temperature dependences at various filling factors. The each curve has a maximum, which decreases and shifts towards higher temperatures with decrease of the filling factor. Such a behavior is also observed at other frequencies.

On the left of the maxima, the temperature dependences of σ_1 are clearly dielectric; in these regions $|\sigma_2| > \sigma_1$. This fact, as well as the frequency dependences of σ_i in the magnetic field interval between 12 and 18 T can be attributed to a pinned mode of WC. On the right of the maxima, $|\sigma_2|$ rapidly decreases with temperature increase. σ_1 also decreases with temperature, but much slower then $|\sigma_2|$, and at high temperatures the condition $|\sigma_2| < \sigma_1$ is valid. Thus, it is natural to ascribe the maximum - the temperature at which the conduction mechanism rapidly changes - to the WC melting point, T_m, for a given filling factor.

So-obtained dependences $T_m(\nu)$ for different frequencies are shown in Fig. 5 as dataset 1. The dataset 2 pre-

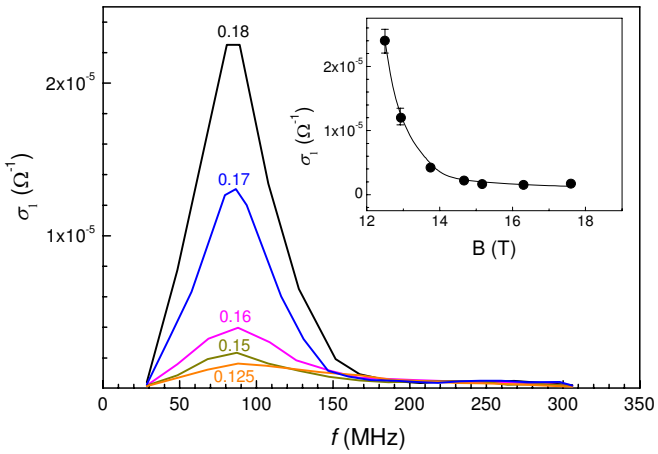

FIG. 3. (Color online) Frequency dependences of σ_1 for different filling factors (shown near the curves). Inset: Magnetic field dependence of σ_1(86 MHz). T=40 mK.

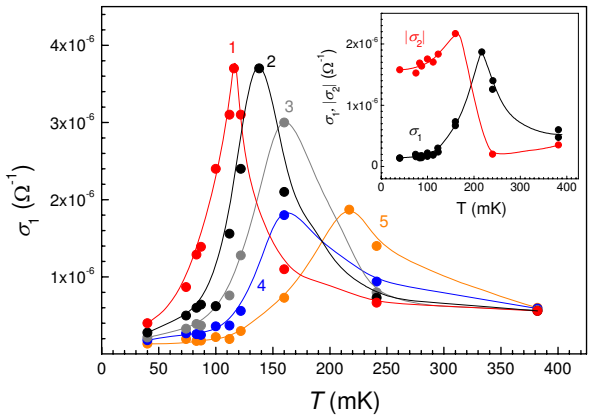

FIG. 4. (Color online) Temperature dependences of σ_1 for different filling factors, ν: 1 - 0.18, 2 - 0.17, 3 - 0.16, 4 - 0.145, 5 - 0.125. $f = 28.5$ MHz. Inset: Temperature dependences of σ_1 and $|\sigma_2|$ for ν= 0.13, $f = 28.5$ MHz. Lines are guides for an eye.

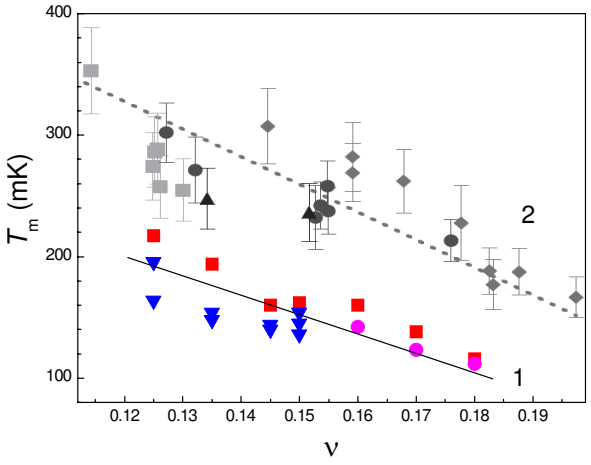

FIG. 5. (Color online) 1 - Dependence of the "melting temperature", T_m, on the filling factor ν for different frequencies, f: ■ - 28.5 MHz, ▼ - 86 MHz, ● - 142 MHz. 2 - Melting temperature, T_m, from Ref. 16 determined as the value where resonances disappear.

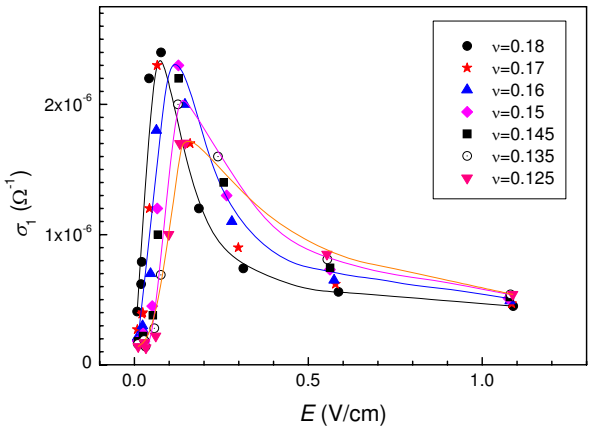

FIG. 6. (Color online) Dependences of σ_1 on the SAW electric field amplitude, E, for different filling factors ν. f = 28.5 MHz, $T = 40$ mK.

sented in the same figure is taken from Ref. 16 where the temperature dependence of the amplitude of the pinning resonance was studied as a function of the filling factor in a GaAs/AlGaAs heterojunction with carrier density tuned by backgate in the range of $n = (1.2 \div 8.1) \times 10^{10}$ cm^{-2}. In Ref. 16, $T_m(\nu)$ was defined as the temperature at which the pinning resonance disappears at a given filling factor ν. Note that the dependences $T_m(\nu)$ obtained in this research and in Ref. 16, i.e., by different procedures, are similar. However, the pinning resonance disappears at higher temperature than the temperature where the conduction mechanism rapidly changes. One can speculate that the melting temperatures determined by different procedures correspond to boundaries of the transition from the Wigner glass to the electron liquid.

C. Results: Nonlinear response

Shown in Fig. 6 are dependences of σ_1 on the amplitude of the electric field, E, produced by the SAW for several filling factors $0.125 \leq \nu \leq 0.18$. The electric field was determined according to Eq. (2) from Ref. 17, see also Ref. 18. The electric field dependences of σ_1 are similar to the temperature dependences shown in Fig. 4. Therefore, increase in the SAW amplitude acts as an increase of the temperature.

The electric field dependences of $|\sigma_2|$ for different ν are shown in Fig. 7. Notice that the dependences $\sigma_2(E)$ for different filling factors collapse on the same curve. For convenience, both components σ_1 and $|\sigma_2|$ at frequency 28.5 MHz and $\nu = 0.125$ are presented in the same graph, see the inset. On the left of the maximum

of $\sigma_1(E)$, $|\sigma_2| > \sigma_1$. This behavior is compatible with the predictions[19] for a Wigner crystal. On the right of the maximum, $|\sigma_2|$ rapidly drops and becomes much less than σ_1. It indicates a change of the AC conduction mechanism. Assuming that an intense SAW increases the temperature of the electron system we ascribe this behavior to melting of the Wigner crystal. The behaviors of $\sigma_{1,2}$ are similar for different frequencies with the exception of the frequency $f = 142$ MHz at which $\sigma_2 > 0$ at all used intensities.

III. DISCUSSION

The behavior of $\sigma(\omega)$ shown in Fig. 2 is typical for a pinned mode of a Wigner crystal,[19–23] see also Refs. 2 and 5 for a review. The crystal manifests itself in observed resonances in $\sigma_1(\omega)$,[24] which has been interpreted as a signature of a solid and explained as due to the pinning mode (the disorder gapped lower branch of the magnetophonon)[6,7,19,20,22] of WC crystalline domains oscillating collectively within the disorder potential. The WC states compete with the fractional quantum Hall effect (FQHE) states. Based on several experiments and calculations it is concluded that at $\nu = 1/5$ the FQHE dominates while at ν slightly less or slightly higher than 1/5 the WC state wins, see, e.g., Fig. 9 from Ref. 2.

The dynamic response of a weakly pinned Wigner crystal at not too small frequencies is dominated by the collective excitations[19,20,23] where an inhomogeneously broadened absorption line (the so-called pinning mode) appears.[6,25] It corresponds to collective vibrations of correlated segments of the Wigner crystal around their equilibrium positions formed by the random pinning potential. The mode is centered at some disorder- and magnetic-field-dependent frequency, ω_p (so-called pinning frequency), with a width being determined by a

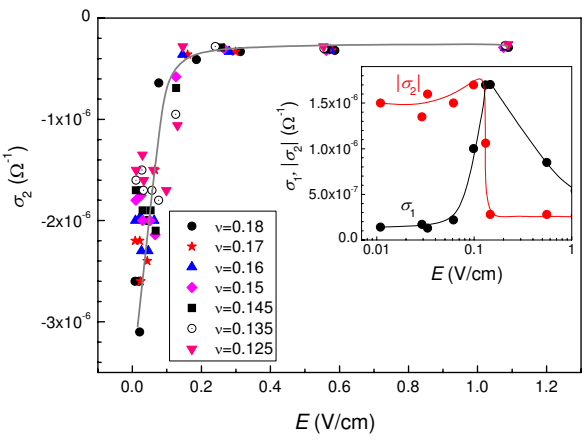

FIG. 7. (Color online) Dependences of $\sigma_2(E)$ for different filling factors ν. Inset: Dependences of σ_1 and $|\sigma_2|$ on the SAW electric field for $\nu = 0.125$. $f = 28.5$ MHz, $T = 40$ mK. Lines are guides for an eye.

complicated interplay between different collective excitations in the Wigner crystal. There are modes of two types: transverse (magnetophonons) and longitudinal (magnetoplasmons). The latter include fluctuations in electron density. An important point is that pinning modifies both modes, and the final result depends on the strength and the correlation length, ξ, of the random potential. Depending in the strength and the correlation length of the random potential, the frequency, ω_p may either increase, or decrease when the magnetic field rises.

The ratio ω_p/ω_c, where ω_c is the cyclotron frequency, can be arbitrary. Depending on the interplay between the ratio ω_p/ω_c and the ratio $\eta \equiv \sqrt{\lambda/\beta}$ between the shear (β) and bulk (λ) elastic moduli of the Wigner crystal, one can specify two regimes where the behaviors of $\sigma^{\rm AC}$ are different:

$$(a)\ 1 \ll \omega_c/\omega_{p0} \ll \eta, \quad (b)\ 1 \ll \eta \ll \omega_c/\omega_{p0}\,. \qquad (1)$$

Here ω_{p0} is the pinning frequency at $B = 0$. As a result, the variety of different behaviors is very rich. Assuming $\xi \gg l_B = (\hbar c/eB)^{1/2}$ one can cast the expression for $\sigma_{xx}(\omega)$ from Ref. 19 into the form

$$\sigma(\omega) = -i\frac{e^2 n\omega}{m^*\omega_{p0}^2}\frac{1 - iu(\omega)}{[1 - iu(\omega)]^2 - (\omega\omega_c/\omega_{p0}^2)^2}\,, \qquad (2)$$

where the function $u(\omega)$ is different for regimes (a) and (b).

Let us consider the regime (b) since only this regime seems to be compatible with our experimental results. Then

$$u(\omega) \sim \begin{cases} (\omega/\Omega)^{2s}, & \omega \ll \Omega\,, \quad (b1) \\ \text{const}, & \Omega \ll \omega \ll \omega_c\,. \quad (b2) \end{cases} \qquad (3)$$

Here $\Omega \sim \omega_{p0}^2\eta/\omega_c$, while s is some critical exponent. According to Ref. 19, $s = 3/2$.

Assuming the regime (b1) we can cast Eq. (2) in the form $\sigma(\omega) \equiv \sigma_0 s(\omega/\Omega)$ where

$$\sigma_0 \equiv \frac{e^2 n\eta^2}{2m^*\omega_c}\,, \quad s(\tilde\omega) = -2\frac{i\tilde\omega(1 - i\tilde\omega^3)}{\eta[(1 - i\tilde\omega^3)^2 - (\eta\tilde\omega)^2]}\,, \qquad (4)$$

with $\tilde\omega = \omega/\Omega$. This function is normalized in order to have its maximum η-independent. Graphs of real and imaginary parts of $s(\omega/\Omega)$ for $\eta = 4$, 5 and 6 are shown in Fig. 8.

Equation (4) predicts decrease of the maximum magnitude of $\sigma_1(\omega)$ with increase of magnetic field. This prediction is compatible with our experiment, see the inset in Fig. 3. However, the predicted behavior of maximum frequency as $\omega_p \propto \omega_c^{-1}$ is not observed – the resonant frequency is almost independent of magnetic field, as seen in Fig. 3. One needs to note, however, that the specificity of our experimental technique does not allow to trace the impact of small change in frequency on the dependence σ on ω.

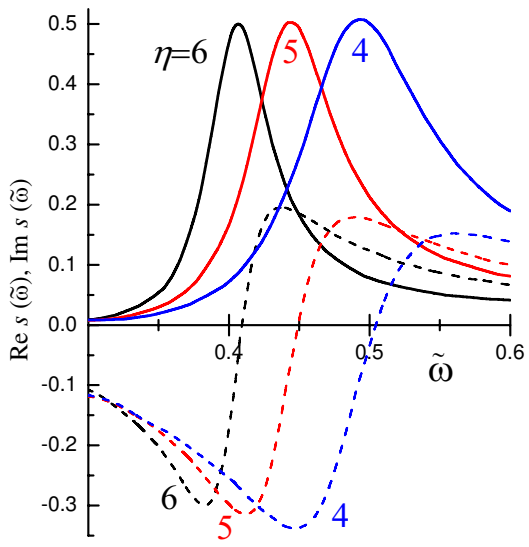

FIG. 8. (Color online) Graphs of Re s (solid lines) and Im s (dash lines) for $\eta = 4$, 5, and 6.

Unfortunately, the experimental data shown in Fig. 2 do not provide an accurate structure of the maximum, and therefore do not allow fitting the model with high accuracy. Assuming $\eta = 5$ that gives approximately correct shape of the curves in Fig. 2 and taking into account that the maximum of $\sigma_1(\omega)$ occurring at $\omega_{\max}/2\pi \approx 86$ MHz corresponds to $\omega/\Omega = 0.44$, we conclude that $\Omega = \omega_{\max}/0.44 \approx 1.2 \times 10^9$ s^{-1}. The quantity $\omega_p \equiv 0.44\Omega_{\max} = 0.44\omega_{p0}^2\eta/\omega_c$ plays the role of the pinning frequency in the magnetic field.[19]

The frequency ω_{p0} can then be determined as

$$\omega_{p0} = \sqrt{\omega_c\Omega/\eta}.$$

Substituting $\eta = 5$, $\Omega = 1.2\times10^9$ s^{-1}, $\omega_c = 3.2\times10^{13}$ s^{-1} ($B = 12.2$ T, $\nu = 0.18$) we obtain

$$\omega_{p0} = 8.7 \times 10^{10} \text{ s}^{-1}.$$

Therefore, the regime (b) of Eq. (1) is the case, as we expected.

Estimating the Larkin length, i.e., the WC domain correlation length, as

$$L = 2\pi c_t/\omega_{p0},$$

where $c_t = (\beta/nm^*)^{1/2} \approx 4 \times 10^6$ cm/s is the velocity of the WC transverse mode for our electron density n we obtain $L \approx 3 \times 10^{-4}$ cm that is much larger than both the distance between the electrons $a = 4.8\times10^{-6}$ cm and the magnetic length $l_B = 7.3 \times 10^{-7}$ cm,

$$L \gg a \gg l_B.$$

These inequalities justify using the theory[19] for our estimates.

In conclusion, we have measured the absorption and the velocity of SAWs in high-mobility samples n-GaAs/AlGaAs in magnetic fields 12÷18 T (i.e., at filling factors $\nu = 0.18 \div 0.125$). From the measurement results the complex AC conductance, $\sigma^{AC}(\omega) \equiv \sigma_1(\omega) - i\sigma_2(\omega)$ was found, and its dependences on frequency, temperature and the amplitude of the SAW-induced electric field were discussed. We conclude that in the studied interval of the magnetic field and $T < 200$ mK the electronic system forms a pinned Wigner crystal, the so-called Wigner glass. The estimate of the correlation (Larkin) length of the Wigner glass is ≈ 3 μm at $B = 12.2$ T.

We have also defined an effective melting temperature, T_m, as the temperature corresponding to the maximum in the temperature dependence of σ_1, or rapid decrease of $|\sigma_2|$. These behaviors indicate a rapid change in the conductance mechanism – from the dielectric behavior at $T < T_m$ to the metallic one at $T > T_m$.

ACKNOWLEDGMENTS

I.L.D. is grateful for support from RFBR via grant 14-02-00232. The authors would like to thank E. Palm, T. Murphy, J.-H. Park, and G. Jones for technical assistance. NHMFL is supported by NSF Cooperative Agreement DMR-1157490 and the State of Florida. The work at Princeton University was funded by the Gordon and Betty Moore Foundation through the EPiQS initiative Grant GBMF4420, and by the National Science Foundation MRSEC Grant DMR-1420541.

[1] E. Wigner, Phys. Rev. **46**, 1002 (1934).
[2] M. Shayegan, "Flatland electrons in high magnetic fields," in *High Magnetic Fields: Science and Technology*, Vol. 3, edited by F. Herlach and N. Miura (World Scientific Co, Singapore, 2006) pp. 31–60, ArXive: cond-mat/0505520v1.
[3] A. I. Larkin and Y. N. Ovchinnikov, J. Low Temp. Phys. **34**, 409 (1979).
[4] H. W. Jiang, H. L. Stormer, D. C. Tsui, L. N. Pfeiffer, and K. W. West, Phys. Rev. B **44**, 8107 (1991).
[5] M. Shayegan, in *Perspectives in Quantum Hall Effects*, edited by S. D. Sarma and A. Pinczuk (Wiley, New York, 1997) Chap. 9.
[6] H. Fukuyama and P. A. Lee, Phys. Rev. B **18**, 6245 (1978).
[7] B. G. A. Normand, P. B. Littlewood, and A. J. Millis, Phys. Rev. B **46**, 3920 (1992).
[8] A. J. Millis and P. B. Littlewood, Phys. Rev. B **50**, 17632

(1994).
[9] I. V. Kukushkin, V. I. Fal'ko, R. J. Haug, K. von Klitzing, K. Eberl, and K. Tötemayer, Phys. Rev. Lett. **72**, 3594 (1994); I. V. Kukushkin, V. I. Fal'ko, R. J. Haug, K. v. Klitzing, and K. Eberl, Phys. Rev. B **53**, R13260 (1996).
[10] H. C. Manoharan, Y. W. Suen, M. B. Santos, and M. Shayegan, Phys. Rev. Lett. **77**, 1813 (1996).
[11] D. C. Glattli, G. Deville, V. Duburcq, F. I. B. Williams, E. Paris, B. Etienne, and E. Y. Andrei, Surf. Sci. **229**, 344 (1990); F. I. B. Williams, P. A. Wright, R. G. Clark, E. Y. Andrei, G. Deville, D. C. Glattli, O. Probst, B. Etienne, C. Dorin, C. T. Foxon, and J. J. Harris, Phys. Rev. Lett. **66**, 3285 (1991).
[12] M. A. Paalanen, R. L. Willett, P. B. Littlewood, R. R. Ruel, K. W. West, L. N. Pfeiffer, and D. J. Bishop, Phys. Rev. B **45**, 11342 (1992).
[13] Y. P. Li, T. Sajoto, L. W. Engel, D. C. Tsui, and M. Shayegan, Phys. Rev. Lett. **67**, 1630 (1991).
[14] I. L. Drichko, I. Yu. Smirnov, A. V. Suslov, L. N. Pfeiffer, K. W. West, and Y. M. Galperin, Solid State Commun. **213-214**, 46 (2015).
[15] I. L. Drichko, A. M. Diakonov, I. Y. Smirnov, Y. M. Galperin, and A. I. Toropov, Phys. Rev. B **62**, 7470 (2000).
[16] Y. P. Chen, G. Sambandamurthy, Z. H. Wang, R. M. Lewis, L. W. Engel, D. C. Tsui, P. D. Ye, L. N. Pfeiffer, and K. W. West, Nature Physics **2**, 452 (2006).
[17] I. L. Drichko, A. M. Dyakonov, I. Yu. Smirnov, and A. I. Toropov, Fiz. Tekh. Poluprovod **34**, 436 (2000), [Semiconductors **34**, 422 (2000)].
[18] I. L. Drichko, A. M. Dyakonov, V. D. Kagan, A. M. Kreshchuk, T. Polyanskaya, I. G. Savelev, I. Yu. Smirnov, and A. V. Suslov, Fiz. Tekh. Poluprovod **31**, 1357 (1997), [Semiconductors **31**, 1170 (1997)].
[19] M. M. Fogler and D. A. Huse, Phys. Rev. B **62**, 7553 (2000).
[20] H. A. Fertig, Phys. Rev. B **59**, 2120 (1999).
[21] H. Yi and H. A. Fertig, Phys. Rev. B **61**, 5311 (2000).
[22] R. Chitra, T. Giamarchi, and P. Le Doussal, Phys. Rev. B **65**, 035312 (2001).
[23] M. M. Fogler, Physica E **22**, 98 (2004).
[24] P. D. Ye, L. W. Engel, D. C. Tsui, R. M. Lewis, L. N. Pfeiffer, and K. West, Phys. Rev. Lett. **89**, 176802 (2002).
[25] H. Fukuyama and P. A. Lee, Phys. Rev. B **17**, 535 (1978).